Proceedings of the 28th IEEE
EMBS Annual International Conference
New York City, USA, Aug 30-Sept 3, 2006

Design of a High Speed Transcutaneous Optical Telemetry Link

D. Michael Ackermann, Jr., Brian Smith, Kevin L. Kilgore, and P. Hunter Peckham

Abstract— **In some neural prosthetic applications there is a need for high bandwidth communication between an implanted device and an external device. For example, transmitting 100 channels of neural waveform data for a cortical prosthetic control system may require up to 40 Mbps for a 100 channel array. Due to the high bandwidth required and its relative immunity from interference, optical telemetry is the most realistic method for achieving a clinically robust transcutaneous communication system capable of achieving these data rates. It is proposed that a transcutaneous optical telemetry link design can be optimized to system level design parameters (power consumption, implant location, etc.) by having a quantified understanding of the different link level design parameters (optical power, lens size, tissue effects, transmitter-receiver alignment, etc.) and an understanding as to how those parameters interact, and will allow for a design guided by an a priori assessment of these parameters. Some of these design factors and their interactions are identified and described. One of these parameters, the tissue optical spatial impulse response is measured empirically for several porcine dermal tissue configurations, and it's implications for device design tradeoffs are discussed.**

I. Introduction

In some neural prosthetic applications there is a need for high bandwidth communication between an implanted device and an external device. For example, recent advances have demonstrated the feasibility of real-time cortical prosthetic control systems [1]-[4]. Currently, these recorded cortical signals must be transmitted from the implanted device to a processing unit external to the body to be processed into a control signal. Transmitting many channels of neural waveform data requires large channel bandwidths (e.g. up to 40 Mbps for a 100 channel array). Other applications may also require high rate transcutaneous data transfer, including cochlear implants, visual prosthetics and cortical stimulation sensory prosthetics.

High rate transcutaneous data transmission can be achieved by several methods, including the use of percutaneous wires, acoustic energy and electromagnetic energy (RF and optical). Optical telemetry may provide the best opportunity for achieving a clinically robust system capable of achieving these data rates.

Optical telemetry is a mature, well established technology: fiber-optic and free-air optical communication systems are common in consumer goods and are quite well understood. Optical telemetry offers two significant advantages over other methods that make it quite attractive for high rate biotelemetry: the optical portion of the EM spectrum is unregulated worldwide for communications purposes, and interference from other sources can be made insignificant (described below in greater detail). Optical telemetry has been used for several transcutaneous communication applications. Low to moderate data rate (9.6 kbps – 1 Mbps) implementations include systems for providing command signals or low rate data to or from neuromuscular stimulators [5], artificial hearts or implanted cardiac assist devices [6]-[8], bladder stimulators [9], laboratory animal monitoring systems [10], neural recording systems [11],[12] and generic communication systems [13]. A higher rate implementation has also been developed, showing the feasibility of high rate optical transcutaneous data transfer at rates of 10-80 Mbps [14]. Some of these systems required relatively large amounts of power to perform successfully (20-70 mW emitter consumption @ 10 Mbps, [14]), which could limit the applicability of an optical link for an implanted system. However, a detailed analysis of the tradeoffs involved in designing a high speed transcutaneous optical telemetry link (TOTL) has not yet been performed. It is proposed that a TOTL design can be optimized to system level design parameters (power consumption, implant location, etc.) by having a quantified understanding of the different link level design parameters (optical power, lens size, tissue effects, transmitter-receiver alignment, etc.) and an understanding as to how those parameters interact, and will allow for a design guided by an a priori assessment of these parameters. Some of these design factors and their interactions are identified and described herein.

II. Procedure And Methods

A. Design Parameters And Their Interactions

The primary system level design constraints and parameters for a TOTL are the data rate of the link, the bit error rate (BER), the implant location, the misalignment tolerance of the transmitter and receiver, the device size, device power consumption, data latency, and safety of the device. These parameters affect each other in quantifiable ways that allow one to assess the tradeoffs between them when designing a TOTL. Many of these factors are directly affected by the link level design parameters described below.

This work was supported by Grant EB-001740 from the National Institutes of Health – Biomedical Imaging and Bioengineering and Grant NS-041809 from the National Institutes of Health – National Institute on Neurological Diseases and Stroke. Principal Investigator P. Hunter Peckham.

The authors are with the Dept. of Biomedical Engineering, Case Western Reserve University and Cleveland FES Center, Cleveland, Ohio 44106 USA (e-mail: dma18@case.edu).

K.L. Kilgore and P.H. Peckham are with MetroHealth Medical Center, Cleveland, Ohio, USA and the Louis Stokes Veterans Affairs Medical Center, Cleveland, Ohio, USA.

Many of these link level design factors interact directly or indirectly through the signal to noise ratio at the input of the receiver, SNR_i. The SNR_i is critical to link performance, as it determines the ability for the receiver decision circuitry to accurately interpret the data (i.e. perform with a low BER). There is an inherent non-linear tradeoff between the BER of the link and the SNR_i for a given data rate, which will partially depend on the characteristics of the receiver [15]. Receiver design has been well documented [15], and this work will focus on the tradeoffs at the optical interface between the transmitter and receiver. Figure 1 shows a block diagram of a TOTL, with the blocks relevant to this analysis highlighted.

Generically, the SNR_i of a link is defined as,

$$SNR_i = \frac{I_S}{I_N} = \frac{P_S R}{I_{N_{elec}} + P_{N_{amb}} R} \quad (1)$$

where I_s and I_N are the photocurrents resulting from incident signal optical power and photodiode noise current respectively, P_s is the received signal optical power, R is the photodiode responsivity (A/W), I_{Nelec} is the input referred noise for the receiver and P_{Namb} is the incident optical power due to interfering light sources (such as ambient light).

P_S can be further defined as

$$P_S = \int_{A_T} P_{Tx} J_{Rx\lambda} \eta_\lambda dA \quad (2)$$

where P_{Tx} (W) is the optical power of the transmitted pulse, $J_{Rx\lambda}$ (cm^{-2}) is the tissue's optical spatial impulse response flux at wavelength λ, η_λ is an efficiency factor ($\eta_\lambda \leq 1$) accounting for any inefficiencies in optics/optical filters at λ and A_T represents the tissue area over which the receiver optics integrate the signal.

The factors that affect the total signal photocurrent and their relationship to system level design parameters include emitter wavelength, emitter optical power, tissue effects, lens size, transmitter-receiver misalignment, receiver noise, ambient light sources, photodiode responsivity, optical domain filtering, receiver signal domain filtering, line coding and photodiode and emitter selection. Each of these parameters can be independently manipulated to ensure that the proper signal strength for a given TOTL design will be achieved.

The emitter wavelength is an important design parameter and should be chosen to maximize power transfer across the skin (minimize absorption and scatter). Skin is an optically turbid media, meaning that it both scatters and absorbs light. The wavelengths in the range of ~800-1300 nm represent the skin's 'optical window,' where absorption and scattering are minimal [16]. Many commercially available emitters and photodiodes are optimized for operation in this range, as this is the same wavelength range used for many fiber optic and free-air applications.

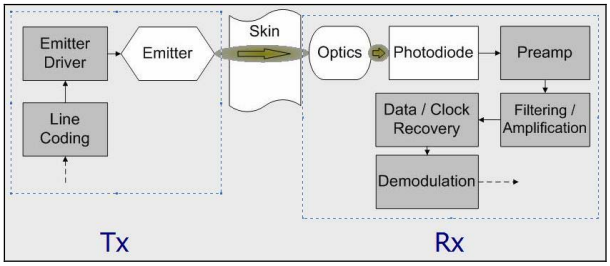

Fig. 1 Block diagram of a TOTL. The highlighted section represents those elements that are relevant to the transmitter-receiver optical interface analysis.

The optical power transmitted from the emitter, P_{Tx}, governs the total electrical power consumed by the emitter, and will vary with emitter type.

$J_{Rx\lambda}$ greatly depends on the presence and thickness of the individual dermal layers (epidermis, dermis and hypodermis\adipose tissue), which vary with anatomical location [17]. $J_{Rx\lambda}$ has not been published for relevant tissue types and was determined empirically for this work.

A_T is governed by the dimensions of the receiver lens and axial misalignment of the transmitter and receiver (i.e. the signal is spatially integrated over the receiver lens area offset from the center of the distribution by the axial misalignment).

The factors that contribute to I_N are I_{Nelec}, which is a function of the receiver electronics, and P_{Namb}. The presence and intensity of interfering light sources that contribute to P_{Namb} can vary greatly depending on environmental conditions and the degree of optical shielding the receiver package provides. Fortunately, P_{Namb} can be significantly reduced with filtering techniques in both the optical and signal domains. Using an optical filter at the receiver that is tuned to the wavelength of the emitter can prevent much of the interfering optical power from ever reaching the photodiode, but may also attenuate the wavelength of interest, reducing η_λ [18]. Most interfering light sources have signal power that consists of frequencies that are significantly lower than those present in the TOTL data stream (Daylight: DC, Fluorescent lights: frequencies up to tens or hundreds of kilohertz), and can therefore be filtered out in the signal domain [19]. R dictates the relative importance of these two factors.

B. Experimental Determination of Tissue Optical Spatial Impulse Response Flux

$J_{Rx\lambda}$ was determined empirically for samples of porcine dermal tissue from 5 animals (41 total samples), consisting of several different dermal layers and thicknesses at λ=850 nm. All samples were comprised of epidermal and dermal layers (combined thickness of approximately 2 mm) and hypodermal/adipose layers of varying thickness (0 mm - ~9.5 mm thick). Total sample thickness (as measured under no applied tension or compression while resting on horizontal surface) varied from approximately 2 to 11.5 mm. All tissue was harvested and analyzed within 24 hours post mortem. A narrow beam light source (Advanced Optical Components HFE 4093-342) was applied to the internal face of each tissue sample, and the distribution of the transmitted optical power on the external face of the tissue was measured by moving a single small-area photodiode over the tissue surface (1mm separation). The position of the photodiode was manipulated using a computer controlled x-y plotter and data acquisition system. Each measured power distribution was made relative to the total transmitted power and divided by the active area of the photodiode, resulting in

a discrete, empirical representation of $J_{Rx\lambda}$ for the tissue sample. These measurements were recorded with DC optical input, but will apply for frequencies relevant to the data rates in question because of the rapid transport of light through tissue [20].

III. Results And Discussion

A. Tissue Spatial Impulse Response

The tissue spatial impulse response, $J_{Rx\lambda}$, was determined for several porcine dermal tissue configurations. Figure 2 shows an empirical flux distribution for a typical 3.5 mm thick sample. The response resembles a Gaussian distribution in shape, and has a volume equal to the total transmittance, T_{tot}, relative to the emitted laser power. The shape of this surface is dependent on the tissue type: increased tissue thickness tends to decrease its height and increase its relative width due to increased scatter and absorption of photons. The inset image in Figure 2 shows a two-dimensional representation of the received optical distribution relative to the distribution of power emitted from the laser. Both the laser and tissue distributions are represented on a log scale in the inset. The laser power is very concentrated within a circular distribution of 0.8 mm diameter. The double peak shown in the laser distribution is due to the wire bond on the laser die.

Figure 3 shows the total transmittance through the tissue as a function of the total tissue thickness. Increased tissue thickness resulted in increased absorption and an approximately exponential decay of total transmittance (R^2 = 0.8049). This data shows that even tissue of ~11.5 mm thickness permits significant power transfer, suggesting that TOTL implant sites may not be limited to locations with thin dermal covering.

Figure 4 shows the full width at half maximum, FWHM, of $J_{Rx\lambda}$ as a function of total tissue thickness. Increased tissue thickness resulted in a linear increase in FWHM due to increased tissue scatter (R^2 = 0.9513). The increase in tissue thickness is due to an increase in hypodermis thickness (mostly adipose tissue) and increased thickness of adipose stores. Adipose tissue is highly scattering, resulting in significant increases in the FWHM with increases in tissue thickness.

The data represented in Figures 3 and 4 show that thinner tissue will allow for the most power efficient TOTL designs due to the larger power transmittance, although the broader power distribution of thicker tissue may soften misalignment tolerances.

B. Effect of Link Design Parameters

Figure 5 shows the effect of circular lens size and axial transmitter-receiver misalignment on P_s relative to the total transmittance for the distribution shown in Figure 2. P_s was determined by simulating a misaligned lens by cutting a circular dissection of the $J_{Rx\lambda}$ volume and integrating under the curve. A tradeoff exists between P_s, lens size and axial

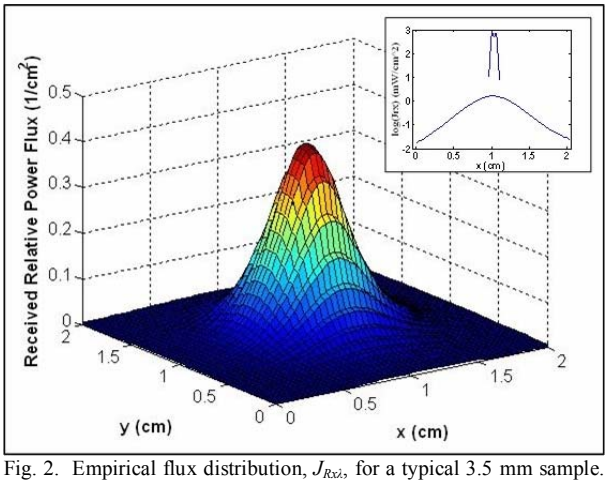

Fig. 2. Empirical flux distribution, $J_{Rx\lambda}$, for a typical 3.5 mm sample. The x and y dimensions represent the two spatial dimensions (2 cm x 2 cm), and the z dimension is the received flux (cm^{-2}) relative to the total input power. The inset image shows $J_{Rx\lambda}$ relative to the emitter power, (log10 scale).

misalignment. Generally, a larger lens will integrate more of the signal, but will require a larger external receiver. Similarly, increasing misalignment will result in less total integrated signal. Lens size and misalignment tolerance can be manipulated to compensate for one another. By knowing the composition of the dermal tissue at the implant site a priori, the affects of the tissue on the TOTL signal strength can be determined and accounted for in the design. Conversely, if implant location is flexible, it could be dictated by the design process. For example, a design with a misalignment tolerance of 0.5 cm using a lens with a radius of 1 cm, and a design with no misalignment tolerance and a lens radius of only 0.5 cm achieve approximately the same optical power at the receiver (79% of T_{tot}, and 74% of T_{tot}, respectively). Approximately the same received optical power (78% of T_{tot}) could also be achieved by allowing a misalignment of 0.5 cm, using a lens of radius 0.5 cm and 7 times the emitted optical power. The same signal power can be achieved using three very different strategies, demonstrating how an a priori assessment of these parameters could guide the design of a TOTL. The system level design constraints (power, misalignment, size, implant location) will dictate how the link level parameters (optical

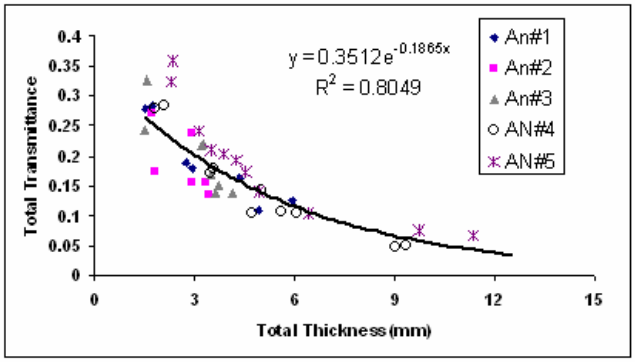

Fig. 3. Total transmittance *Ttot*, through the tissue as varies with total tissue thickness (~0.5 mm epidermis + ~2 mm dermis + 0 – ~9 mm adipose tissue).

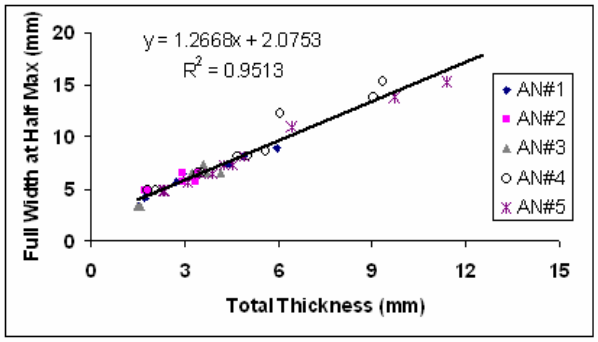

Fig. 4. FWHM of J_{Rxl} as varies with total tissue thickness (~0.5 mm epidermis + ~2 mm dermis + 0 – ~9 mm adipose tissue).

power, misalignment tolerance, lens size) are to be optimized.

C. Other Factors Affecting Power Consumption

Several other important factors affect the power consumption of the TOTL, including the data line code (how the digital data is encoded into the transmitted bits), photodiode selection, emitter selection and device safety (which places a ceiling on optical power output). The line code can be manipulated to improve power efficiency by choosing codes that trade bandwidth (which can be very large for an optical link) for power efficiency. The photodiode used should have a high R and be as small as possible (lower capacitance to drive) without exceeding the saturation limit for the photodiode (ambient power can be limited with optical fiters). Saturation limits and R will also vary with the semiconductor type. Electrical-to-optical power efficiencies vary widely with emitter type, with Vertical-Cavity Surface-Emitting Laser, VCSEL, emitters being quite power efficient in general (e.g. Advanced Optical Components HFE 4093-342).

IV. Conclusion

This ongoing work demonstrates that an understanding of the link design parameters and their interactions is possible, and that this understanding can be used to guide an a priori design for a low power transcutaneous optical telemetry link. Work on such a link is currently in progress.

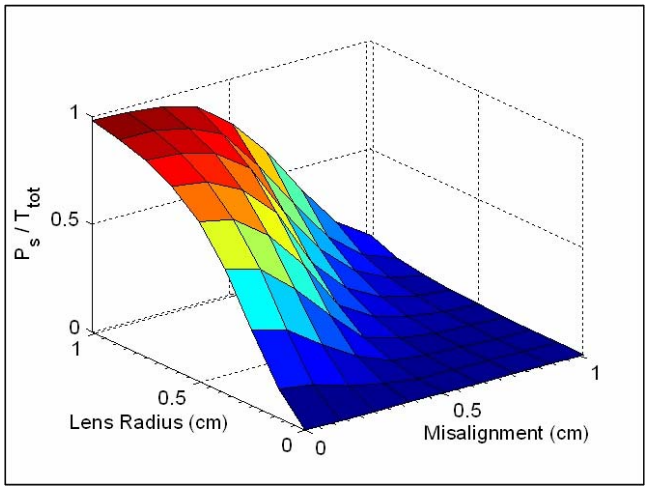

Fig. 5 Effect of receiver lens radius and axial misalignment of transmitter and receiver on total power integrated by the lens relative to the total transmittance.

References

[1] J. K. Chapin, K.A. Moxon, R.S. Markowitz, M.A.L. Nicolelis "Real-time control of a robot arm using simultaneously recorded neurons in the motor cortex," *Nature*, vol. 2, no. 7, 1999.

[2] S. Tillery, D. M. Taylor, R. Issacs, "Online control of a prosthetic arm from motor control signals" *Soc. For Neurosci. Abst.*, vol. 26, 2000.

[3] M.D. Serruya, N.G. Hatsopoulos, L. Paninski, M.R. Fellows, J.P. Donoghue, "Brain-machine interface: instant neural control of a movement signal," *Nature*, vol. 416, pp. 141-142, 2002.

[4] D. M. Taylor, S.I. Tillery, A.B. Schwartz, "Direct Cortical Control of 3-D Neuroprosthetic Devices," *Science*, vol. 296, no. 5574, pp. 1829-1832, 2002.

[5] J. Jarvis, S. Salmons, "A family of neuromuscular stimulators with optical transcutaneous control," *Journal of Medical Engineering and Technology*, vol. 15, no. 2, pp. 53-57, 1991.

[6] Y. Mitamura, E. Okamoto, M. Tomohisa, "A transcutaneous optical information transmisión system for implantable motor-driven artificial hearts," *ASAIO Transactions*, vol. 36, pp. M278-M280, 1990.

[7] J.A. Miller, G. Belanger, I. Song, F. Johnson, "Transcutaneous optical telemetry system for an implantable electrical ventricular heart assist devive," *Med. & Biol. Eng. & Comput.*, vol. 30, pp. 370-372, 1992.

[8] K.I. Inoue, et al., "Transcutaneous optical telemetry system using laser diode," *Japanese Journal of Artificial Organs*, vol. 27, no. 2, pp. 363-367, 1998.

[9] M. Sawan, K. Arabi, B. Provost, "Implantable volume monitor and miniaturized stimulator dedicated to bladder control," *Artificial Organs*, vol. 21, no. 3, pp. 219-222, 1997.

[10] N. Kudo, K. Shimizu, G. Matsumoto, "Fundamental study on transcutaneous biotelemetry using diffused light," *Frontiers Med. Biol. Eng.*, vol. 1, no. 1, pp. 19-28, 1988.

[11] K. Goto, T. Nakagawa, "Transcutaneous photocoupler for transmission of biological signals," *Optics Letters*, vol. 27, no. 20, pp. 1797-1799, 2002.

[12] B.C. Larson, "An optical telemetry system for wireless transmission of biomedical signals across the skin," Ph.D. dissertation, Dept. Elect. Eng., Massachusetts Institute of Technology, Cambridge, MA, 1999.

[13] J.L. Abita, W. Schneider, "Transdermal optical communications," *Johns Hopkins APL Technical Digest*, vol. 25, no. 3, pp. 261-268, 2004.

[14] K.S. Guillory, A.K. Misener, A. Pungor, "Hybrid rf/ir transcutaneous telemetry for power and high-bandwidth data," in *2004 Proc. IEEE Engineering in Medicine and Biology Conf.*, pp. 4338-4340, 2004.

[15] B.P. Lathi, *Modern Digital and Analog Communication Systems, 3rd Edition.* New York, NY: Oxford University Press, 1998, Chapters 13-14.

[16] T. Vo-Dinh, *Biomedical Photonics.* Boca Raton, FL: CRC Press, 1998, Chapters 2-3.

[17] C.Y.Tan, B. Statham, R. Marks, P.A. Payne, "Skin thickness measurement by pulsed ultrasound: its reproducibility, validation and variability," *British Journal of Dermatology*, vol. 106, pp. 657-667, 1982.

[18] J.M. Kahn, J.R. Barry, "Wireless infrared communications," *Proceedings of the IEEE*, vol. 85, no. 2, pp. 265-298, 1997.

[19] A.J.C. Moreira, R.T. Valadas, A.M. de Oliveira Duarte, "Optical interference produced by artificial light," *Wireless Networks*, vol. 3, pp. 131-140, 1997.

[20] G. Hausler, J.M. Herrmann, R. Kummer, M.W. Lindner, "Observation of light propagation in volume scatterers with 10^{11}-fold slow motion," *Optics Letters*, vol. 21, no. 14, pp. 1087-1089, Jul 1996.